

Statistical discrimination of lithofacies from pre-stack seismic data constrained by well log rock physics: Application to a North Sea turbidite system.

Per Avseth^{*1}, Tapan Mukerji¹, Gary Mavko¹, and Tor Veggeland²

¹Rock Physics Laboratory, Dept. of Geophysics, Stanford University, CA 94305.

²Norsk Hydro ASA, Vækerø, Norway.

Summary

We present a methodology for predicting lithofacies from seismic amplitudes, and apply it to a North Sea turbidite system. We define *seismic lithofacies* as seismic scale sedimentary units with characteristic rock physics properties. Sonic, gamma ray and density logs are used as training data in a multivariate statistical analysis to objectively determine seismic lithofacies. We classify lithofacies for 7 wells in the area, and create cumulative distribution functions (cdfs) of seismic properties for each facies. Pore fluid variations are accounted for by applying Biot-Gassmann theory. The well log derived cdfs show that unconsolidated thick-bedded clean sands with water, plane laminated thick-bedded sands with oil, and pure shales have very similar acoustic impedance distributions. However, the V_p/V_s -ratio resolves these ambiguities. We therefore conduct AVO analysis to predict seismic lithofacies from seismic data. We assess uncertainties in AVO response related to the inherent natural variability of each lithofacies using a Monte-Carlo technique. AVO probability plots show that there are overlaps between different facies, but the most likely responses for each facies are nicely separated. Zero-offset reflectivity versus AVO-gradient bivariate probability plots are created to better assess the overlap between the different facies. We then analyze real CDP-gathers at several well locations, and successfully predict the seismic lithofacies indicated by the log data. This demonstrates the feasibility of AVO analysis to predict seismic lithofacies. By analyzing a selected 2-D AVO attribute section across the submarine fan lobe, we successfully predict the transition from water-saturated marginal interbedded sand-shales to oil-saturated thick-bedded sands in the center of the lobe/lobe-channel. In general, we find that the turbidite system is a point-sourced sub-marine fan with cemented clean sands indicated in the feeder-channel, uncemented clean sands in the lobe-channels, and interbedded sand-shale facies and shaly sands in interchannel and marginal areas.

Introduction

Deep water clastic systems and associated turbidite reservoirs are often characterized by very complex sand distributions. Reservoir description based on conventional seismic and well-log stratigraphic analysis may be very uncertain in these depositional

environments. Relating lithofacies to rock properties improves the ability to use seismic amplitude information for reservoir prediction and characterization in these systems, as facies have a major control on reservoir geometries and porosity distributions. A turbidite system located in South Viking Graben, North Sea, has been studied. The turbidite sands represent the Heimdal Formation of Late Paleocene age and include an oil field of economic interest (Figure 1).

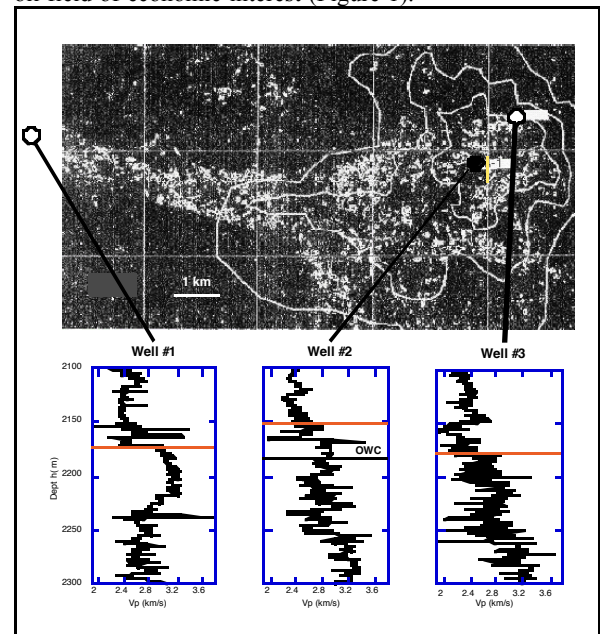


Figure 1: Seismic amplitude map (above) of Top Heimdal Formation, corresponding to the gray lines in the well logs (P-wave velocity) (below). The three wells penetrate a submarine fan in the feeder channel (well #1), in a lobe-channel (well #2) and in the marginal area of the lobe (well #3). The Heimdal Formation dramatically changes character between the wells.

First we define seismic lithofacies and classify them in 7 different wells using multivariate statistical analysis based on training data selected from one of the wells. Then we extract cumulative distribution functions (cdf) for each of the facies. The cdfs generate the basis for uncertainty analysis in AVO response, and for predicting the most likely lithofacies from seismic data.

Seismic lithofacies prediction

Seismic lithofacies

A *seismic lithofacies* is a seismically resolvable or significant sedimentary unit characterized by its lithology (clay content), bedding configuration (massive, interbedded or chaotic), petrography (grain size, clay location and cementation) and seismic properties (P-wave velocity, S-wave velocity and density) (Avseth, 1998). In the turbidite system studied, we recognize the following siliciclastic lithofacies: thick bedded sands (facies II), interbedded sand-shale units (facies III), silt-laminated or silty shales (facies IV), and pure shales (facies V). 3 sub-facies of facies II are observed and honor seismically important petrographic variations within the thick-bedded sand facies: II_a) cemented massive sands, II_b) unconsolidated massive sands, and II_c) plane laminated sands.

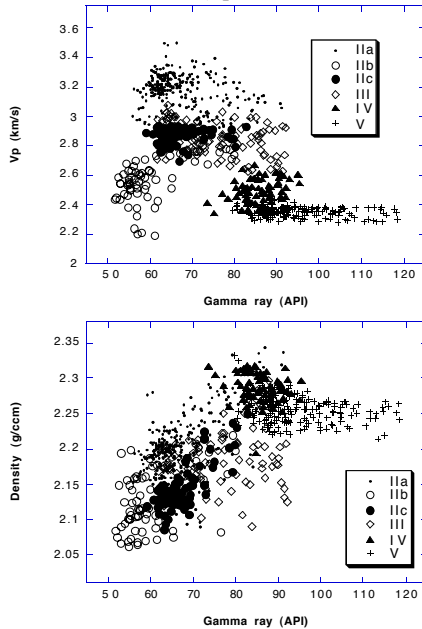


Figure 2: P-wave velocity versus gamma ray (above) and density versus gamma ray (below), for different seismic lithofacies in training data (i.e. well #2). Note the ambiguity in P-wave velocity between facies IIb and IV/V.

Well #2 is selected as a type well for identification of seismic lithofacies from well log data. Primarily, we have used the gamma ray log to determine the different facies, as it represents a good clay indicator. However, density, and sonic logs have also been used to ensure a reliable facies analysis of this well. The sub-facies IIb and IIc have been determined from core, thin-section and SEM analyses, whereas IIa, representing a zone where no cores were taken, has been diagnosed as cemented thick-bedded sands using rock physics theory (c.f. Avseth et

al., 1998). Figure 2 shows the different seismic lithofacies plotted as P-wave velocity vs. gamma ray, and density vs. gamma ray. S-wave velocity would be an additional important log to be used in the classification, but we had S-wave information in only 2 of the wells.

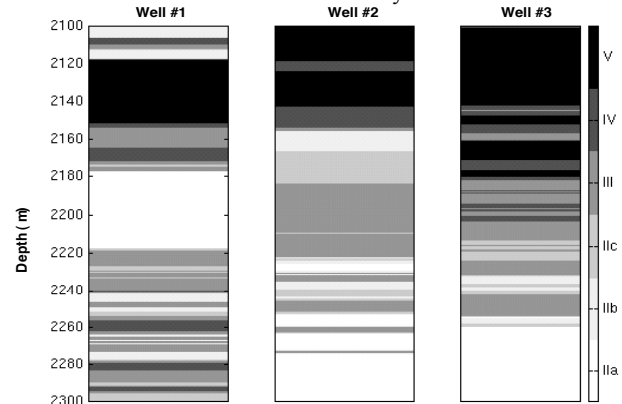


Figure 3: Seismic lithofacies classification results. The channel sands in well # 1 are classified as cemented (IIa), whereas the marginal lobe facies encountered in well # 3 are identified as interbedded sands-shales (facies III).

Multivariate statistical classification of seismic lithofacies from well logs

The log data from the type well are used as training data for a multivariate statistical classification of seismic lithofacies in other wells. Gamma ray, Vp and density are the three parameters we use in our classification. We only needed to use gamma ray and Vp to do this classification, but density was used to double-check that our classification was correct, and to help reveal the potential presence of non-siliciclastic lithologies (e.g. limestone, marl, volcanic ash fall deposits etc.). However, we did not encounter non-siliciclastic facies in the wells used in the classification. Only the depth interval from 2100-2300m was included in the analysis for each well, in order to avoid depth effects (i.e. pressure) when analyzing seismic properties. Figure 3 shows the classification results in wells # 1-3, where only gamma ray and P-wave velocity logs were used. This classification was done in 7 wells.

AVO uncertainty analysis

Based on the facies classification, we extract cumulative density functions of seismic properties for each of the lithofacies, and for oil-saturated sand facies (Figure 4). The oil-saturated cdfs were calculated from the water-saturated cdfs using Biot-Gassmann theory. As we observe the Vp/Vs ratio to be a much better lithofacies and pore-fluid indicator than acoustic impedance, we conclude that AVO analysis must be employed to predict lithofacies from seismic data.

Seismic lithofacies prediction

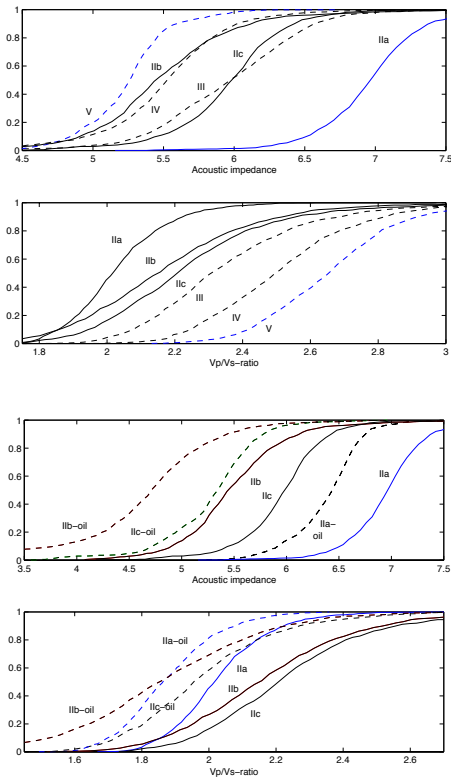


Figure 4: Cumulative distribution functions (cdfs) of acoustic impedance and Vp/Vs ratio for each facies (the 2 upper plots), and for oil versus brine saturation in the sandy facies (the 2 lower plots). We observe a much better discrimination in Vp/Vs ratio than in acoustic impedance, both in terms of lithofacies and in terms of pore fluids.

Based on the cdfs of velocities and density, we can assess the uncertainties in AVO response related to the natural variability within each lithofacies. Figure 5 shows the derived probability density functions (pdfs) of AVO response for facies IIa and IIb with and without oil, capped by a silty shale (facies IV), which is the most common cap-rock observed above the Heimdal Formation in the area of study. The plots have been generated from the Monte-Carlo simulated seismic properties drawn randomly from the lithofacies cdfs. We made sure the simulation honored the correlation between the three parameters. Reflectivities were calculated using Aki and Richards (1980) approximation of Zoeppritz equations.

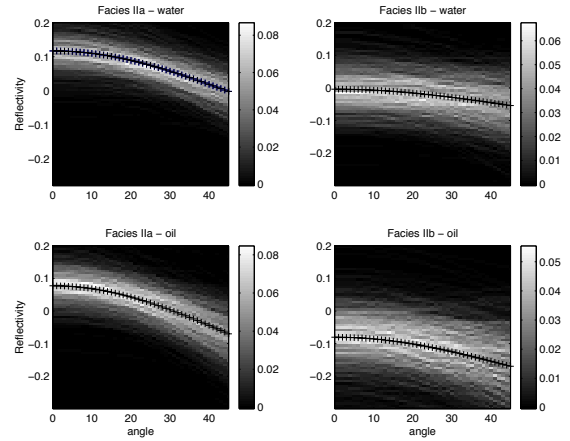


Figure 5: AVO pdfs for facies IIa and IIb with brine and oil, assuming facies IV as cap-rock. There are relatively large uncertainties in AVO response related to the variability within each facies, and there are overlaps between different facies, and pore fluid scenarios. However, the most likely AVO responses are distinct for each facies and pore fluid scenario. The superimposed black ticked lines represent the deterministic AVO response calculated from the median values of the cdfs.

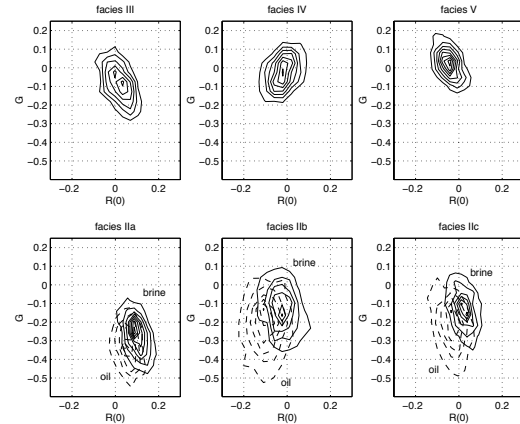


Figure 6: Bivariate distribution of the different seismic lithofacies in R(0)-G plane, with facies IV as cap-rock.

To better assess the uncertainties in reflectivity for different facies and pore fluids, we generated bivariate probability plots (Figure 6) of zero-offset reflectivity (R0) vs. AVO gradient (G). The center of each contour plot represents the most likely R(0) and G for each facies.

Real data analysis

Figure 7 shows the real CDP gathers at the three well locations in Figure 1, and the corresponding picked amplitudes at the Top Heimdal horizon superimposed on exact Zoeppritz reflectivity curves from the well log data.

Seismic lithofacies prediction

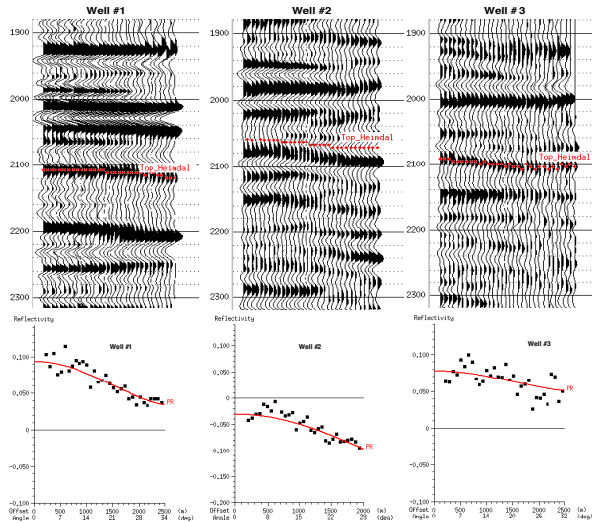


Figure 7: CDP-gathers and AVO curves for wells # 1-3.

In well 2 we know that the Top Heimdal sands are unconsolidated, oil-saturated sands, and are capped by silty shales. The corresponding AVO response is a negative zero offset reflectivity and negative AVO gradient. In well #1, we have a water-saturated cemented sand below a silty shale. The corresponding AVO response in well #1 shows a strong positive zero-offset reflectivity and a relatively strong negative gradient. Finally, in well #3 we observe a moderate positive zero-offset reflectivity and a moderate negative gradient, corresponding to interbedded sand-shale facies capped by silty shales. Hence, we observe 3 distinct AVO responses in the 3 different wells. We conclude that the AVO signature within our turbidite system is controlled by the seismic lithofacies as well as the porefluids. These results demonstrate the feasibility of AVO as a tool to predict lithofacies from seismic data.

Next we use pre-stack seismic information to predict the most likely facies present immediately beneath the Top Heimdal horizon. Assuming a consistent cap-rock (facies IV) is valid as the overlying Lista Formation is normally represented by hemipelagic shales. Figure 8 shows a 2-D seismic stack section across the lobe in figure 1, intersecting the type-well (well #2). Included in this figure are the extracted $R(0)$ and G values along the interpreted Top Heimdal horizon, and the predicted most likely seismic lithofacies. We predict a transition from shales and inter-bedded sand-shales at the margin, to oil-saturated sands (I Ib and IIc) in the center of the lobe. The facies IIb with oil is correctly predicted at the well. The predicted pure shales within the lobe is questionable and could be due to tuning effects or noise. In our subsequent work we will analyze the impact of difference in seismic and log scales on the pdfs.

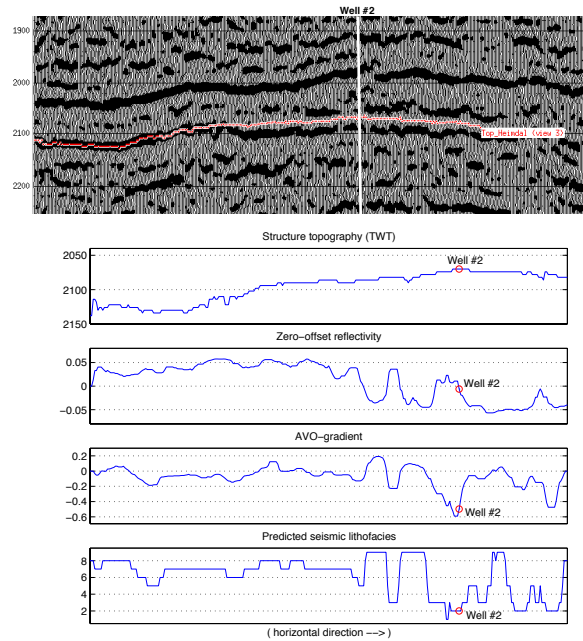


Figure 8: 2-D seismic stack section intersecting well #2 (above). The different curves include: structural topography of Top Heimdal (TWT), zero-offset reflectivity, AVO-gradient and most likely seismic lithofacies along the cross section at the picked horizon. (1-3=IIa-IIc with oil; 4-6=IIa-IIc; 7-9=III-V).

Conclusion

By integrating geophysical and statistical methods, we have shown how we can predict lithofacies from seismic amplitudes in complex turbidite reservoirs.

Acknowledgments

This study was supported by Norsk Hydro ASA who provided the data, and Stanford Rock Physics Project.

References

- Aki, K., and Richards, P. G., 1980: Quantitative Seismology, Freeman W. H. & Co.
- Avseth, P., 1998: Seismic lithofacies in North Sea deep-water clastic systems, expanded abstract, AAPG conference, Salt Lake City, May 1998.
- Avseth, P., Dvorkin, J., Mavko, G., and Rykkje, J., 1998: Diagnosing high-porosity sands for reservoir characterization using sonic and seismic, Abstract submitted for SEG, New Orleans, Sept., 1998.